Simultaneous reconstruction of shape and impedance in corrosion detection

Fioralba Cakoni*, Rainer Kress† and Christian Schuft†

Abstract

Corrosion detection can be modelled by the Laplace equation for an electric or a heat potential in a simply connected planar domain D with a homogeneous impedance boundary condition on a non-accessible part of the boundary ∂D. We consider the inverse problem to simultaneously recover the non-accessible part of the boundary and the impedance function from two pairs of Cauchy data on the accessible part of the boundary. Our approach extends the method proposed by Kress and Rundell [16] for the corresponding problem to recover the interior boundary curve of a doubly connected planar domain and is based on our previous work on reconstruction of the impedance function for a known shape or the shape for a known impedance function [4, 5]. Based either on a potential approach or on a Green's integral formulation the inverse problem is equivalent to a system of nonlinear and ill-posed integral equations that can be solved iteratively by linearization. We will present the mathematical foundation of the method and, in particular, establish injectivity for the linearized system at the exact solution. Numerical reconstructions will show the feasibility of the method.

1 Introduction

We consider an inverse problem that models corrosion detection. Let $D \subset \mathbb{R}^2$ be a simply connected bounded domain with piece-wise smooth boundary ∂D. By ν we denote the outward unit normal to ∂D. We assume that the boundary is composed of $\partial D = \overline{\Gamma}_m \cup \overline{\Gamma}_c$ where Γ_m and Γ_c are two connected open disjoint portions of ∂D of class C^2 without cusps at the two intersection points. The electrostatic or

*Department of Mathematical Sciences, University of Delaware, Newark, Delaware 19716, USA
†Institut für Numerische und Angewandte Mathematik, Universität Göttingen, 37083 Göttingen, Germany

heat potential u in a conducting medium D with a non-accessible boundary part Γ_c affected by corrosion is modeled by the following boundary value problem

$$\Delta u = 0 \quad \text{in } D, \tag{1.1}$$

$$u = f \quad \text{on } \Gamma_m, \tag{1.2}$$

$$\frac{\partial u}{\partial \nu} + \lambda u = 0 \quad \text{on } \Gamma_c, \tag{1.3}$$

where λ is a nonnegative L^∞ function on Γ_c which can be interpreted as the corrosion coefficient and f is the imposed voltage or temperature, i.e., the Dirichlet data on the accessible boundary part Γ_m. The resulting (and measured) current or heat flux, i.e., the Neumann data on Γ_m is denoted by

$$g = \frac{\partial u}{\partial \nu} \quad \text{on } \Gamma_m. \tag{1.4}$$

For a detailed discussion of this model and related inverse problems we refer to Kaup and Santosa [11], Kaup, Santosa and Vogelius [12] and Inglese [10] and for a recent bibliography to Fasino and Inglese [8]. The inverse problem we are concerned with in this paper is to determine both the shape of Γ_c and the impedance function λ from two pairs (f_1, g_1) and (f_2, g_2) of Cauchy data according to (1.1)–(1.4).

To formulate the boundary value problem (1.1)–(1.3) and the inverse problem more precisely we recall the definitions of some Sobolev spaces (see [17]). Let $\Gamma \subset \partial D$ be a generic open subset of the boundary. If $H^1(D)$ denotes the usual Sobolev space and $H^{1/2}(\partial D)$ its usual trace space, then we define

$$\begin{aligned}
&H^{1/2}(\Gamma) := \{u|_\Gamma : u \in H^{1/2}(\partial D)\},\\
&\widetilde{H}^{1/2}(\Gamma) := \{u \in H^{1/2}(\Gamma) : \operatorname{supp} u \subseteq \overline{\Gamma}\},\\
&H^{-1/2}(\Gamma) := (\widetilde{H}^{1/2}(\Gamma))' \text{ the dual space of } \widetilde{H}^{1/2}(\Gamma),\\
&\widetilde{H}^{-1/2}(\Gamma) := (H^{1/2}(\Gamma))' \text{ the dual space of } H^{1/2}(\Gamma).
\end{aligned}$$

Note that the extension by zero of functions in $\widetilde{H}^{1/2}(\Gamma)$ to the whole of ∂D belongs to $H^{1/2}(\partial D)$ (which is not the case in general for elements in $H^{1/2}(\Gamma)$). The norm on $H^{1/2}(\Gamma)$ is given by

$$\|u\|_{H^{1/2}(\Gamma)} = \inf\{\|v\|_{H^{1/2}(\partial D)} : v \in H^{1/2}(\partial D),\, v|_\Gamma = u\}$$

and the following chain of inclusion holds

$$\widetilde{H}^{1/2}(\Gamma) \subset H^{1/2}(\Gamma) \subset L^2(\Gamma) \subset \widetilde{H}^{-1/2}(\Gamma) \subset H^{-1/2}(\Gamma).$$

It is known [3, 9] that for $f \in H^{1/2}(\Gamma_m)$ there exists a unique solution $u \in H^1(D)$ of (1.1)–(1.3). Hence we can formulate the inverse problem as follows: given two

pairs $f_1, f_2 \in H^{1/2}(\Gamma_m)$ and $g_1, g_2 \in H^{-1/2}(\Gamma_m)$, determine Γ_c and a nonnegative L^∞ function λ on Γ_c such that the unique solutions $u_j \in H^1(D)$ of (1.1)–(1.3) with Dirichlet data $u_j = f_j$ on Γ_m satisfy $\partial u_j/\partial\nu = g_j$ on Γ_m for $j = 1, 2$.

As a preparatory version of this inverse shape and impedance problem, in [4, 5] we considered the inverse shape problem where we reconstructed only the shape assuming λ to be known as a function of the parameter describing the boundary part Γ_c. In general, for direct and inverse boundary value problems in potential theory one has the choice between two complementary solution methods via boundary integral equations: the potential approach and the direct approach via Green's representation theorem. In [4], by two of us, it was suggested to solve the inverse shape problem using an approach based on a single-layer potential with a density on ∂D leading to a system of nonlinear and ill-posed integral equations that is equivalent to the inverse shape problem and can be solved using regularized iterations. As the complimentary approach, in [5] we derived another equivalent system of nonlinear and ill-posed integral equations based on Green's representation theorem. This second approach extends a method suggested by Kress and Rundell [16] to determine the shape of a perfectly conducting inclusion in a homogeneous background from a pair of Cauchy data on the accessible exterior boundary. The inverse problem to simultaneously recover the shape and impedance of an inclusion was recently considered by Rundell in [20] where, in particular, an algorithm was proposed which also can be considered as extension of [16]. It is the aim of the current paper to extend the analysis of [4, 5] to the simultaneous inverse shape and impedance problem for the case of corrosion detection.

The question of uniqueness for the inverse shape and impedance problem was addressed by Bacchelli [2] who established that two pairs of Cauchy data on Γ_m, that is, (f_1, g_1) and (f_2, g_2) uniquely determine both the shape of the domain D and the impedance function λ on ∂D provided that f_1 and f_2 are linearly independent and one of them, say f_1, is positive. In a recent paper Pagani and Pierotti [18] extended this analysis.

The plan of the paper is as follows. In section 2 we will derive our systems of integral equations and prove equivalence to the inverse shape and impedance problem in a Sobolev space setting. However, the ill-posedness of the inverse problem suggests to treat these systems in an L^2 setting that is appropriate for quantifying measurement errors on the data g in the image space and the discussion of the Tikhonov regularization for their stabilization. After describing the linearization and the iteration scheme for the inverse shape and impedance problem in section 3 we show injectivity of the linearization at the exact solution using two Cauchy pairs. Whereas for the Green's representation approach, the local injectivity result is a straightforward extension of the corresponding theorem from [5] for shape reconstruction alone, it is a completely new result in the case of the single-layer potential

approach. For the latter case in [4] local injectivity was only considered for the limiting case $\lambda = \infty$ of a Dirichlet boundary condition. The paper is concluded with some numerical examples for simultaneous shape and impedance reconstructions.

2 Nonlinear integral equations

In this section we present the equivalent systems of integral equations that we employ for the solution of the inverse problem. We begin by noting that the inverse problem is closely related to the following Cauchy problem: Given the pair $f \in H^{1/2}(\Gamma_m)$ and $g \in H^{-1/2}(\Gamma_m)$ find $\alpha \in H^{1/2}(\Gamma_c)$ and $\beta \in H^{-1/2}(\Gamma_c)$ such that there exists a harmonic function $u \in H^1(D)$ satisfying

$$u = f \quad \text{and} \quad \frac{\partial u}{\partial \nu} = g \quad \text{on } \Gamma_m$$

and $u = \alpha$ and $\partial u/\partial \nu = \beta$ on Γ_c. Note that this Cauchy problem admits at most one solution and is known to be ill-posed. Our two solution methods for the Cauchy problem are based on Green's representation theorem and on a single-layer potential approach, respectively. They provide alternatives to the numerous approaches that have been developed in the literature (see e.g. [1], [4] and the references therein).

For the presentation of these two methods, in terms of the fundamental solution

$$\Phi(x, y) = \frac{1}{2\pi} \ln \frac{1}{|x - y|}, \quad x \neq y,$$

we introduce the single- and double-layer potential operators

$$S : H^{-1/2}(\partial D) \to H^{1/2}(\partial D) \quad \text{and} \quad K : H^{1/2}(\partial D) \to H^{1/2}(\partial D)$$

defined by

$$(S\varphi)(x) := \int_{\partial D} \Phi(x, y)\varphi(y)\, ds(y), \quad x \in \partial D, \tag{2.1}$$

and

$$(K\varphi)(x) := \int_{\partial D} \frac{\partial \Phi(x, y)}{\partial \nu(y)}\, \varphi(y)\, ds(y), \quad x \in \partial D, \tag{2.2}$$

as well as their restrictions to the boundary portions given by

$$(S_{kj}\varphi)(x) := \int_{\Gamma_k} \Phi(x, y)\varphi(y)\, ds(y), \quad x \in \Gamma_j, \tag{2.3}$$

and

$$(K_{kj}\varphi)(x) := \int_{\Gamma_k} \frac{\partial \Phi(x, y)}{\partial \nu(y)}\, \varphi(y)\, ds(y), \quad x \in \Gamma_j, \tag{2.4}$$

for $k, j = m, c$.

2.1 Green's theorem approach

From now on, without loss of generality because of the possibility of scaling, we assume that there exists a point $x_0 \in D$ such that $|x - x_0| \neq 1$ for all $x \in \partial D$. Then Theorem 3.16 in [13] guarantees that the operator S defined by (2.1) is injective which is essential for the validity of the converse part of the following theorem taken from [5]. We note that its statements are immediate consequences of Green's representation theorem for harmonic functions.

Theorem 2.1 *Let $\alpha \in H^{1/2}(\Gamma_c)$ and $\beta \in H^{-1/2}(\Gamma_c)$ be a solution to the Cauchy problem. Then there exist $\varphi \in H^{1/2}(\partial D)$ and $\psi \in H^{-1/2}(\partial D)$ such that*

$$\frac{\varphi}{2} + K\varphi - S\psi = 0 \tag{2.5}$$

and φ and ψ have restrictions $\varphi|_{\Gamma_m} = f$, $\varphi|_{\Gamma_c} = \alpha$ and $\psi|_{\Gamma_m} = g$, $\psi|_{\Gamma_c} = \beta$, respectively. Conversely, for any solution $\varphi \in H^{1/2}(\partial D)$ and $\psi \in H^{-1/2}(\partial D)$ of (2.5) satisfying $\varphi|_{\Gamma_m} = f$ and $\psi|_{\Gamma_m} = g$ we have that $\alpha := \varphi|_{\Gamma_c}$ and $\beta := \psi|_{\Gamma_c}$ is a solution of the Cauchy problem.

Corollary 2.2 *The inverse shape and impedance problem is equivalent to solving*

$$\frac{\varphi_i}{2} + K\varphi_i - S\psi_i = 0, \quad i = 1, 2, \tag{2.6}$$

for Γ_c, $\varphi_i|_{\Gamma_c}$, $\psi_i|_{\Gamma_c}$ and λ under the constraints $\varphi_i|_{\Gamma_m} = f_i$, $\psi_i|_{\Gamma_m} = g_i$ and

$$\psi_i|_{\Gamma_c} + \lambda\varphi_i|_{\Gamma_c} = 0$$

for $i = 1, 2$.

The question of existence of a solution to the ill-posed integral equation (2.6) as stated in Corollary 2.2, that is, a characterization of two Cauchy pairs (f_1, g_1) and (f_2, g_2) for which a solution to the inverse shape and impedance problem exists, is the wrong question to ask since, in general, it cannot be answered. Instead of this, assuming that we have correct data or small perturbations thereof, for a stable numerical solution regularization schemes need to be applied. Since the L^2-norm is the appropriate norm to measure the data error, it is natural to consider the equation in L^2 spaces rather than in the trace spaces that are appropriate only for the corresponding forward problems. Hence, for the remainder of the paper we will assume that the data f_i and g_i are in $L^2(\Gamma_m)$ and look for solutions of (2.6) with $\varphi_i|_{\Gamma_c}$ and $\psi_i|_{\Gamma_c}$ in $L^2(\Gamma_c)$.

To simplify notations, in terms of the given Cauchy data we define the combined single- and double-layer potentials

$$w_i(x) := \int_{\Gamma_m} \left\{ f_i(y) \, \frac{\partial \Phi(x, y)}{\partial \nu(y)} - g_i(y)\Phi(x, y) \right\} ds(y), \quad x \in \mathbb{R}^2 \setminus \overline{\Gamma}_m, \; i = 1, 2. \tag{2.7}$$

Then, after separating and renaming the unknowns, in view of Corollary 2.2 we solve the inverse shape and impedance problem by a regularized solution Γ_c, λ and $\varphi_1, \varphi_2 \in L^2(\Gamma_c)$ of the system of integral equations

$$\frac{\varphi_i}{2} + K_{cc}\varphi_i + S_{cc}(\lambda\varphi_i) = -w_i|_{\Gamma_c} \quad i = 1, 2, \tag{2.8}$$

and

$$K_{cm}\varphi_i + S_{cm}(\lambda\varphi_i) = -w_i|_{\Gamma_m}, \quad i = 1, 2, \tag{2.9}$$

where $w_i|_{\Gamma_m}$ in (2.9) represents the limit obtained by approaching Γ_m from outside D. Clearly, these equations are nonlinear with respect to Γ_c. For convenience we note that

$$w_i|_{\Gamma_c} = K_{mc}f_i - S_{mc}g_i \quad \text{and} \quad w_i|_{\Gamma_m} = \frac{f_i}{2} + K_{mm}f_i - S_{mm}g_i.$$

For the further investigation of the integral equations and, in particular, for their numerical solution a parameterization is required. For the sake of simplicity we confine ourselves to smooth boundaries ∂D of class C^2, that is, we represent

$$\partial D = \{z(t) : t \in [0, 2\pi]\} \tag{2.10}$$

with a 2π periodic C^2-smooth function $z : \mathbb{R} \to \mathbb{R}^2$ such that z is injective on $[0, 2\pi)$ and satisfies $z'(t) \neq 0$ for all t. Without loss of generality we may assume that Γ_c and Γ_m are given by

$$\Gamma_c = \{z(t) : t \in (0, \pi)\}, \qquad \Gamma_m = \{z(t) : t \in (\pi, 2\pi)\}.$$

From now on we denote

$$z_c := z|_{(0,\pi)} \quad \text{and} \quad z_m := z|_{(\pi,2\pi)}.$$

Setting $\psi = \varphi \circ z_c$ we obtain from (2.3) and (2.4) the parameterized integral operators

$$(\widetilde{S}_{cj}\psi)(t) = \frac{1}{2\pi}\int_0^\pi \ln\frac{1}{|z_j(t) - z_c(\tau)|}\,|z_c'(\tau)|\psi(\tau)\,d\tau \tag{2.11}$$

and

$$(\widetilde{K}_{cj}\psi)(t) = \frac{1}{2\pi}\int_0^\pi \frac{[z_c'(\tau)]^\perp \cdot [z_j(t) - z_c(\tau)]}{|z_j(t) - z_c(\tau)|^2}\,\psi(\tau)\,d\tau + \frac{\delta_{cj}}{2}\psi(t) \tag{2.12}$$

for $t \in [0, 2\pi]$ and $j = m, c$. Here we used the notation $a^\perp = (a_2, -a_1)$ for any vector $a = (a_1, a_2)$, that is, $a^\perp$ is obtained by rotating a clockwise by 90 degrees, and the convention $\delta_{j\ell} = 1$ if $j = \ell$ and $\delta_{j\ell} = 0$ if $j \neq \ell$ for $j, \ell = c, m$. For the explicit

parameterized form of the combined single- and double-layer potentials $w_{ij} = w_i \circ z_j$ evaluated on Γ_j, $j = c, m$, corresponding to (2.11) and (2.12) we refer to [5].

With the identification of $\lambda = \lambda \circ z_c$ the parameterized form of the equations (2.8) and (2.9) now reads

$$\widetilde{K}_{cc}\psi_i + \widetilde{S}_{cc}(\lambda\psi_i) = -w_{ic}, \quad i = 1, 2, \tag{2.13}$$

and

$$\widetilde{K}_{cm}\psi_i + \widetilde{S}_{cm}(\lambda\psi_i) = -w_{im}, \quad i = 1, 2. \tag{2.14}$$

2.2 Potential approach

We now proceed with nonlinear integral equations based on an alternative solution method for the Cauchy problem by a single-layer potential approach

$$u(x) = \int_{\partial D} \Phi(x, y)\varphi(y)\, ds(y), \quad x \in D, \tag{2.15}$$

with a density $\varphi \in H^{-1/2}(\partial D)$. After defining the normal derivative operator

$$K' : H^{-1/2}(\partial D) \to H^{-1/2}(\partial D)$$

by

$$(K'\varphi)(x) := \int_{\partial D} \frac{\partial \Phi(x, y)}{\partial \nu(x)}\, \varphi(y)\, ds(y), \quad x \in \partial D, \tag{2.16}$$

and recalling our assumption that there exists a point $x_0 \in D$ such that $|x - x_0| \neq 1$ for all $x \in \partial D$, we can state the following theorem.

Theorem 2.3 *Let $\alpha \in H^{1/2}(\Gamma_c)$ and $\beta \in H^{-1/2}(\Gamma_c)$ be a solution to the Cauchy problem. Then there exists $\varphi \in H^{-1/2}(\partial D)$ such that*

$$\begin{aligned} S\varphi &= f \quad \text{on } \Gamma_m, \\ K'\varphi + \frac{\varphi}{2} &= g \quad \text{on } \Gamma_m, \end{aligned} \tag{2.17}$$

and u defined by (2.15) has the restrictions $u|_{\Gamma_m} = f$, $u|_{\Gamma_c} = \alpha$ and $\partial u/\partial\nu|_{\Gamma_m} = g$, $\partial u/\partial\nu|_{\Gamma_c} = \beta$, respectively. Conversely, for any solution $\varphi \in H^{-1/2}(\partial D)$ of (2.17) we have that $\alpha = u|_{\Gamma_c}$ and $\beta = \partial u/\partial\nu|_{\Gamma_c}$ with $u \in H^1(D)$ defined by (2.15) provide a solution to the Cauchy problem.

Proof. Let $u \in H^1(D)$ correspond to a solution to the Cauchy problem. Clearly, $u|_{\Gamma_m} = f$, $u|_{\Gamma_c} = \alpha$ and $\partial u/\partial\nu|_{\Gamma_m} = g$, $\partial u/\partial\nu|_{\Gamma_c} = \beta$. Now we represent u by (2.15) with a density $\varphi \in H^{-1/2}(\partial D)$. By approaching the boundary ∂D from inside D we obtain (2.17) with the aid of the jump relations.

Conversely, if $\varphi \in H^{-1/2}(\partial D)$ solves (2.17) clearly u defined by (2.15) is an $H^1(D)$ solution of the Laplace equation. Furthermore, approaching the boundary ∂D from inside D the system (2.17) yields that $u|_{\Gamma_m} = f$ and $\partial u/\partial \nu|_{\Gamma_m} = g$. Hence, $\alpha = u|_{\Gamma_c}$ and $\beta = \partial u/\partial \nu|_{\Gamma_c}$ provide a solution to the Cauchy problem. □

Corollary 2.4 *The inverse shape and impedance problem is equivalent to solving*

$$\begin{aligned} S\varphi_i &= f_i \quad \text{on } \Gamma_m, \quad i = 1, 2, \\ K'\varphi_i + \frac{\varphi_i}{2} &= g_i \quad \text{on } \Gamma_m, \quad i = 1, 2, \end{aligned} \tag{2.18}$$

and

$$K'\varphi_i + \frac{\varphi_i}{2} + \lambda S\varphi_i = 0 \quad \text{on } \Gamma_c, \quad i = 1, 2, \tag{2.19}$$

for $\Gamma_c, \varphi_1, \varphi_2$ *and* λ.

Since again the question of existence of a solution to the ill-posed integral equations stated in Corollary 2.4 is the wrong question to ask, in the context of regularization methods we will assume that the data f_i and g_i are in $L^2(\Gamma_m)$ and we look for solutions of (2.18)–(2.19) with φ_i in $L^2(\partial D)$.

We recall the boundary parameterization (2.10) and set $\psi = |z'|\,(\varphi \circ z)$. Then we obtain from (2.1) and (2.16) the parameterized integral operators

$$(\widetilde{S}\psi)(t) = \frac{1}{2\pi} \int_0^{2\pi} \ln \frac{1}{|z(t) - z(\tau)|}\, \psi(\tau)\, d\tau$$

and

$$(\widetilde{K}'\psi)(t) = -\frac{1}{2\pi|z'(t)|} \int_0^{2\pi} \frac{[z'(t)]^\perp \cdot [z(t) - z(\tau)]}{|z(t) - z(\tau)|^2}\, \psi(\tau)\, d\tau + \frac{\psi(t)}{2|z'(t)|}$$

for $t \in [0, 2\pi]$. After the identifications $\lambda = \lambda \circ z$ on $[0, \pi]$, $f_i = f_i \circ z$ and $g_i = g_i \circ z$ on $[\pi, 2\pi]$ for $i = 1, 2$ the parameterized form of the system (2.18)–(2.19) reads

$$\begin{aligned} \widetilde{S}\psi_i &= f_i \quad \text{on } [\pi, 2\pi], \\ \widetilde{K}'\psi_i &= g_i \quad \text{on } [\pi, 2\pi] \end{aligned} \tag{2.20}$$

and

$$\widetilde{K}'\psi_i + \lambda \widetilde{S}\psi_i = 0 \quad \text{on } [0, \pi] \tag{2.21}$$

for $i = 1, 2$.

3 Iterative solution

3.1 Green's theorem approach

We now turn to the iteration scheme for solving the system (2.13)–(2.14) and start by linearizing the equations with respect to ψ_1, ψ_2, λ and Γ_c (note that the integral operators are linear with respect to $\psi_i, i = 1, 2$, and λ). This leads to

$$\begin{aligned} &\widetilde{K}_{cc}(\psi_i, z_c) + \widetilde{K}_{cc}(\chi_i, z_c) + d\widetilde{K}_{cc}(\psi_i, z_c; \zeta) \\ &+\widetilde{S}_{cc}(\lambda\psi_i, z_c) + \widetilde{S}_{cc}(\lambda\chi_i, z_c) + d\widetilde{S}_{cc}(\lambda\psi_i, z_c; \zeta) + \widetilde{S}_{cc}(\mu\psi_i, z_c) \\ &= -w_{ic} - \zeta \cdot (\operatorname{grad} w_i) \circ z_c, \quad i = 1, 2, \end{aligned} \tag{3.1}$$

and

$$\begin{aligned} &\widetilde{K}_{cm}(\psi_i, z_c) + \widetilde{K}_{cm}(\chi_i, z_c) + d\widetilde{K}_{cm}(\psi_i, z_c; \zeta) \\ &+\widetilde{S}_{cm}(\lambda\psi_i, z_c) + \widetilde{S}_{cm}(\lambda\chi_i, z_c) + d\widetilde{S}_{cm}(\lambda\psi_i, z_c; \zeta) + \widetilde{S}_{cm}(\mu\psi_i, z_c) \\ &= -w_{im}, \quad i = 1, 2. \end{aligned} \tag{3.2}$$

Here, we have indicated the dependence of the operators both on the density and the boundary parameterization. The operators $d\widetilde{K}_{cc}, d\widetilde{K}_{cm}, d\widetilde{S}_{cc}, d\widetilde{K}_{cm}$ denote the Fréchet derivatives with respect to z_c in direction ζ of the operators $\widetilde{K}_{cc}, \widetilde{K}_{cm}, \widetilde{S}_{cc}, \widetilde{K}_{cm}$, respectively. They are obtained by formally differentiating the kernels of the integral operators with respect to z_c (see [19]) and for their explicit representation we refer to [5]. Note that the perturbation ζ is different from zero only on Γ_c.

Solving the inverse shape and impedance problem via equations (3.1)–(3.2) can be summarized by the following algorithm:

1. We make an initial guess for the non-accessible boundary part Γ_c, parameterized by z_c, and for the impedance function λ. Then we find the densities ψ_1 and ψ_2 for the two pairs of Cauchy data (f_1, g_1) and (f_2, g_2) by solving (2.13).

2. Given an approximation for z_c, ψ_1, ψ_2 and λ, the linear system (3.1) and (3.2) is solved for ζ, χ_1, χ_2 and μ to obtain the update $z_c + \zeta$ for the parameterization, $\psi_1 + \chi_1, \psi_2 + \chi_2$ for the boundary values and $\lambda + \mu$ for the impedance.

3. The second step is repeated until a suitable stopping criterion is satisfied.

Clearly, the ill-posedness requires to incorporate a regularization in order to achieve stability. For this, we propose Tikhonov regularization with a Sobolev

penalty term on the parameterization as well as on the impedance and an L^2 penalty term on the boundary values.

For the following results on injectivity of the linearization (3.1)–(3.2) at the exact solution we need some assumptions on the regularity of the solution u on the boundary. We assume that the exact solution u is continuous on $\overline{\Gamma}_c$ and twice continuously differentiable on Γ_c such that $\psi = u \circ z_c$ satisfies

$$t^\delta(\pi - t)^\delta |\psi'(t)| \le c, \quad 0 < t < \pi, \tag{3.3}$$

for some positive constants c and $\delta < 1$. In view of the regularity results for the direct problem (see [7]) this regularity assumption is not too restrictive. We also assume that Γ_c is of class C^3 to ensure that $\zeta = q[z_c']^\perp \in C^2[0,\pi]$ for a scalar function $q \in C^2[0,\pi]$. (Recall that ∂D is assumed to be of class C^2.)

Theorem 3.1 *Let z_c be the parameterization of Γ_c, let $\psi_1, \psi_2 \in C^1[0,\pi] \cap C^2(0,\pi)$ satisfy the condition* (3.3) *and the integral equations* (2.13)–(2.14) *for a nonnegative $\lambda \in C[0,\pi]$ and linearly independent Dirichlet data f_1 and f_2. Then for any solution $\zeta = q[z_c']^\perp \in C^2[0,\pi]$, $\chi_1, \chi_2 \in L^2[0,\pi]$ and $\mu \in C[0,\pi]$ to the homogeneous system*

$$\begin{aligned} \widetilde{K}_{cc}(\chi_i, z_c) + d\widetilde{K}_{cc}(\psi_i, z_c; \zeta) + \widetilde{S}_{cc}(\lambda\chi_i, z_c) + d\widetilde{S}_{cc}(\lambda\psi_i, z_c; \zeta) \\ + \widetilde{S}_{cc}(\mu\psi_i, z_c) + \zeta \cdot (\operatorname{grad} w_i) \circ z_c = 0, \quad i = 1, 2, \end{aligned} \tag{3.4}$$

and

$$\begin{aligned} \widetilde{K}_{cm}(\chi_i, z_c) + d\widetilde{K}_{cm}[\psi_i, z_c; \zeta] + \widetilde{S}_{cm}(\lambda\chi_i, z_c) + d\widetilde{S}_{cm}(\lambda\psi_i, z_c; \zeta) \\ + \widetilde{S}_{cm}(\mu\psi_i, z_c) = 0, \quad i = 1, 2, \end{aligned} \tag{3.5}$$

we have that $\chi_1 = \chi_2 = 0, \zeta = 0$ and $\mu = 0$.

Proof. Analogous to [5, Theorem 4.4] it can be shown that

$$\chi_i = -|z'|\lambda q \psi_i \tag{3.6}$$

and

$$[q\psi_i']' + |z'|^2\lambda(\lambda + \kappa)q\psi_i - \mu\psi_i|z'| = 0 \tag{3.7}$$

for $i = 1, 2$, where κ denotes the curvature of Γ_c. Note, that the additional term $\mu\psi_i|z'|$ in (3.7), as compared to [5], is due to the jump $\mu\psi_i$ of the normal derivative of the single-layer potential

$$\int_0^\pi \mu(\tau)\psi_i(\tau)\Phi(x, z_c(\tau))|z_c'(\tau)|\, d\tau, \quad x \in \mathbb{R}^2 \setminus \overline{\Gamma}_c.$$

This potential corresponds to the additional operators $\widetilde{S}_{cc}(\mu\psi_i, z_c)$ and $\widetilde{S}_{cm}(\mu\psi_i, z_c)$ in the homogeneous system (3.4)–(3.5) (compared to the system for the inverse shape problem as treated in [5]). Linearly combining (3.7) for ψ_1 and ψ_2 we find

$$\psi_2[q\psi_1']' - \psi_1[q\psi_2']' = 0$$

and from this as in [5, Theorem 4.8] we can conclude $q = 0$. (We note that in this step the assumption (3.3) is essential.) Then (3.6) implies that $\chi_1 = \chi_2 = 0$.

Now, by (3.7) we conclude that also $\mu\psi_i|z'| = 0$ for $i = 1, 2$. An application of Holmgren's theorem and the homogeneous impedance boundary condition (1.3) for u_i on Γ_c lead to the conclusion that u_i cannot vanish on an open subset of Γ_c. Therefore, in view of $\psi_i = u_i \circ z_c$, it follows that $\mu = 0$. □

3.2 Potential approach

Based on Corollary 2.4 now we present a second iteration scheme for solving the inverse shape and impedance problem that is obtained by linearizing the parameterized equations (2.20)–(2.21) with respect to ψ_1, ψ_2, λ and Γ_c. This leads to

$$\begin{aligned} \widetilde{S}(\psi_i, z) + \widetilde{S}(\chi_i, z) + d\widetilde{S}(\psi_i, z; \zeta) &= f_i \quad \text{on } [\pi, 2\pi], \\ \widetilde{K}'(\psi_i, z) + \widetilde{K}'(\chi_i, z) + d\widetilde{K}'(\psi_i, z; \zeta) &= g_i \quad \text{on } [\pi, 2\pi], \end{aligned} \tag{3.8}$$

and

$$\begin{aligned} &\widetilde{K}'(\psi_i, z) + \widetilde{K}'(\chi_i, z) + d\widetilde{K}'(\psi_i, z; \zeta) \\ &\quad + \lambda\{\widetilde{S}(\psi_i, z) + \widetilde{S}(\chi_i, z) + d\widetilde{S}(\psi_i, z; \zeta)\} + \mu\widetilde{S}(\psi_i, z) = 0 \quad \text{on } [0, \pi] \end{aligned} \tag{3.9}$$

for $i = 1, 2$. Here, the operators $d\widetilde{K}'$ and $d\widetilde{S}$ denote the Fréchet derivatives with respect to z in direction ζ of the operators $\widetilde{K}'$ and $\widetilde{S}$, respectively. Again, they are obtained by formally differentiating the kernels of the integral operators with respect to z and are given by

$$d\widetilde{S}(\psi, z; \zeta)(t) = \frac{1}{2\pi} \int_0^{2\pi} \frac{[z(\tau) - z(t] \cdot [\zeta(t) - \zeta(\tau)]}{|z(t) - z(\tau)|^2} \, \psi(\tau) \, d\tau, \quad t \in [0, 2\pi], \tag{3.10}$$

and

$$\begin{aligned} &d\widetilde{K}'(\psi, z; \zeta)(t) \\ &= \frac{1}{2\pi|z'(t)|} \int_0^{2\pi} \left\{ \frac{2[z'(t)]^\perp \cdot [z(t) - z(\tau)] \, [z(t) - z(\tau)] \cdot [\zeta(t) - \zeta(\tau)]}{|z(t) - z(\tau)|^4} \right. \\ &\quad \left. - \frac{[z'(t)]^\perp \cdot [\zeta(t) - \zeta(\tau)] + [\zeta'(t))]^\perp \cdot [z(t) - z(\tau)]}{|z(t) - z(\tau)|^2} \right\} \psi(\tau) \, d\tau \\ &\quad - \frac{z'(t) \cdot \zeta'(t)}{|z'(t)|^2} \widetilde{K}'(\psi, z)(t), \quad t \in [0, 2\pi]. \end{aligned} \tag{3.11}$$

Recall that the perturbation ζ is different from zero only on Γ_c.

Solving the inverse shape and impedance problem via equations (3.8)–(3.9) can be summarized by the following algorithm:

1. We make an initial guess for the non-accessible boundary part Γ_c, parameterized by z_c, and for the impedance function λ. Then we find the densities ψ_1 and ψ_2 for the two pairs of Cauchy data (f_1, g_1) and (f_2, g_2) by solving (2.20).

2. Given an approximation for z_c, ψ_1, ψ_2 and λ, the linear system (3.8)–(3.9) is solved for ζ, χ_1, χ_2 and μ to obtain the update $z_c + \zeta$ for the parameterization, $\psi_1 + \chi_1, \psi_2 + \chi_2$ for the densities and $\lambda + \mu$ for the impedance.

3. The second step is repeated until a suitable stopping criterion is satisfied.

Again, the ill-posedness requires the incorporation of a regularization in order to achieve stability and as above we propose Tikhonov regularization with a Sobolev penalty term on the parameterization and on the impedance and an L^2 penalty term on the densities.

To establish a result on local injectivity we require some preparations. As above we assume that Γ_c is of class C^3.

For $\psi \in H^1[0, 2\pi]$ and $\zeta \in C[0, 2\pi]$ we define

$$v(x) := \int_0^{2\pi} \psi(\tau)\Phi(x, z(\tau))\, d\tau \tag{3.12}$$

and

$$V(x) := -\int_0^{2\pi} \psi(\tau)\, \mathrm{grad}_x\, \Phi(x, z(\tau)) \cdot \zeta(\tau)\, d\tau \tag{3.13}$$

for $x \in D$.

Lemma 3.2 *For $\psi \in H^1[0, 2\pi]$ and ζ of the form $\zeta = q[z']^\perp$ with $q \in C[0, 2\pi]$ such that $q|_{[0,\pi]} \in C^2[0, \pi]$ and $q|_{[\pi,2\pi]} = 0$ we have that*

$$d\widetilde{S}(\psi, z; \zeta) = V \circ z + |z'| q(\mathrm{grad}\, v \cdot \nu) \circ z. \tag{3.14}$$

Proof. This follows straightforwardly from the jump relations for single–layer potentials.

Lemma 3.3 *Under the assumptions of Lemma 3.2 we have that*

$$d\widetilde{K}'(\psi, z; \zeta) = |z'|\, \kappa\, q\, (\mathrm{grad}\, v \cdot \nu) \circ z - \frac{1}{|z'|}\, \frac{d}{dt}\, q\, \frac{d}{dt}\, (v \circ z) + (\mathrm{grad}\, V \cdot \nu) \circ z \tag{3.15}$$

where κ denotes the curvature of ∂D.

PROOF. The operators $\widetilde{K}$ and $\widetilde{K}'$ are adjoint in the sense of

$$\int_0^{2\pi} \psi\, \widetilde{K}(\varphi, z)\, dt = \int_0^{2\pi} |z'|\, \varphi\, \widetilde{K}'(\psi, z)\, dt$$

for all $\varphi, \psi \in H^1[0, 2\pi]$. From this, differentiating with respect to z in direction ζ, we find that

$$\int_0^{2\pi} \psi\, d\widetilde{K}(\varphi, z; \zeta)\, dt = \int_0^{2\pi} \left\{ |z'|\, \varphi\, d\widetilde{K}'(\psi, z; \zeta) + \frac{z' \cdot \zeta'}{|z'|}\, \varphi\, \widetilde{K}'(\psi, z) \right\} dt \tag{3.16}$$

for all $\varphi, \psi \in H^1[0, 2\pi]$. We use the representation

$$d\widetilde{K}(\varphi, z; \zeta)(t) = \int_0^{2\pi} \varphi'(\tau)\ \operatorname{grad}_x \Phi(z(t), z(\tau)) \cdot \{[\zeta(\tau)]^\perp - [\zeta(t)]^\perp\}\, d\tau, \quad t \in [0, 2\pi],$$

from equation (4.8) in the proof of Lemma 4.1 in [5] (where due to periodicity the terms at the end points of the interval cancel). Interchanging the order of integration we obtain

$$\int_0^{2\pi} \psi\, d\widetilde{K}(\varphi, z; \zeta)\, dt = \int_0^{2\pi} \varphi'(t) \int_0^{2\pi} \operatorname{grad}_x \Phi(z(t), z(\tau)) \cdot \{[\zeta(\tau)]^\perp - [\zeta(t)]^\perp\}\, \psi(\tau)\, d\tau\, dt.$$

After a partial integration, together with (3.16) this implies

$$\begin{aligned} &|z'(t)|\, d\widetilde{K}'(\psi, z; \zeta)(t) + \frac{z'(t) \cdot \zeta'(t)}{|z'(t)|}\, \widetilde{K}'(\psi, z)(t) \\ &= \frac{d}{dt} \int_0^{2\pi} \operatorname{grad}_x \Phi(z(t), z(\tau)) \cdot \{[\zeta(t)]^\perp - [\zeta(\tau)]^\perp\}\, \psi(\tau)\, d\tau. \end{aligned} \tag{3.17}$$

In view of $\zeta = q\,[z']^\perp$, that is, $\zeta^\perp = -q\, z'$, using the jump relations for the derivative of single-layer potentials, we compute

$$\int_0^{2\pi} \operatorname{grad}_x \Phi(z(t), z(\tau)) \cdot [\zeta(t)]^\perp\, \psi(\tau)\, d\tau = -q(t)\, \frac{d}{dt}\, v(z(t)). \tag{3.18}$$

A further partial integration yields

$$\int_0^{2\pi} \operatorname{grad}_x \Phi(z(t), z(\tau)) \cdot [\zeta(\tau)]^\perp\, \psi(\tau)\, d\tau = -\int_0^{2\pi} \frac{d}{d\tau}\, [q(\tau)\psi(\tau)]\ \Phi(z(t), z(\tau))\, d\tau$$

whence, from Maue's formula for the normal derivative of double-layer potentials (see also equation (4.9) in the proof of Lemma 4.1 in [5]) it follows that

$$\frac{d}{dt} \int_0^{2\pi} \operatorname{grad}_x \Phi(z(t), z(\tau)) \cdot [\zeta(\tau)]^\perp\, \psi(\tau)\, d\tau = -|z'(t)|\, (\operatorname{grad} V \cdot \nu)(z(t)). \tag{3.19}$$

Finally, from the jump relations for the normal derivative of single-layer potentials, we note that

$$\frac{z' \cdot \zeta'}{|z'|} \, \widetilde{K}'(\psi, z) = -\kappa \, |z'|^2 \, q \, (\operatorname{grad} v \cdot \nu) \circ z \tag{3.20}$$

where for the curvature κ we have used the expression

$$\kappa = \frac{z'' \cdot [z']^{\perp}}{|z'|^3} \, .$$

Now, combining (3.17)–(3.20) yields the assertion (3.15). □

Lemma 3.4 *Let ψ solve (2.20)–(2.21) for a nonnegative $\lambda \in C[0, \pi]$ and let the single-layer potential u with density ψ satisfy the condition (3.3). Assume that ζ is of the form given in Lemma 3.2 and that $\chi \in L^2[0, 2\pi]$, $\mu \in C[0, \pi]$ and ζ solve the homogeneous system*

$$\begin{aligned} \widetilde{S}(\chi, z) + d\widetilde{S}(\psi, z; \zeta) = 0 \quad & \text{on } [\pi, 2\pi], \\ \widetilde{K}'(\chi, z) + d\widetilde{K}'(\psi_i, z; \zeta) = 0 \quad & \text{on } [\pi, 2\pi] \end{aligned} \tag{3.21}$$

and

$$\begin{aligned} \widetilde{K}'(\chi, z) + d\widetilde{K}'(\psi, z; \zeta) + \lambda \widetilde{S}(\chi, z) \\ + \lambda d\widetilde{S}(\psi, z; \zeta) + \mu \widetilde{S}(\psi, z) = 0 \quad \text{on } [0, \pi]. \end{aligned} \tag{3.22}$$

Then

$$[q(u \circ z)']' + |z'|^2 \lambda(\lambda + \kappa) q (u \circ z) - \mu (u \circ z) \, |z'| = 0. \tag{3.23}$$

If $q = 0$ on Γ_c then $\chi = 0$.

Proof. Recalling definition (3.12), we identify $u = v$ and note that u satisfies the impedance boundary condition (3.3) since ψ solves (2.20)–(2.21). We define

$$V_0(x) := \int_0^{2\pi} \chi(\tau) \Phi(x, z(\tau)) \, d\tau$$

for $x \in D$ and set

$$W := V_0 + V.$$

Then, in view of $\zeta = 0$ on Γ_m, combining (3.14), (3.15) and (3.21) we observe that $W = 0$ and $\partial W / \partial \nu = 0$ on Γ_m. Hence, Holmgren's theorem implies that $W = 0$ in D.

From Lemma 3.2 and 3.3, the integral equation (3.22) and $W = 0$ in D we conclude that

$$\frac{1}{|z'|}\,[q(u\circ z)']' - |z'|(\lambda+\kappa)q(\operatorname{grad} u\cdot\nu)\circ z - \mu u\circ z$$

$$= -d\widetilde{K}'(\psi_i,z;\zeta) + (\operatorname{grad} V\cdot\nu)\circ z - \lambda\, d\widetilde{S}(\psi_i,z;\zeta) + \lambda\, V\circ z - \mu S(\psi,z)$$

$$= \widetilde{K}'(\chi,z) + (\operatorname{grad} V\cdot\nu)\circ z + \lambda(\widetilde{S}(\chi,z) + V\circ z) = (\operatorname{grad} W\cdot\nu)\circ z + \lambda(W\circ z) = 0.$$

The differential equation (3.23) now follows by observing the impedance boundary condition (1.3) for the solution u.

If $q = 0$ on Γ_c then $W = V_0$. Now $V_0 = 0$ in D implies $\chi = 0$ because of the injectivity of $\widetilde{S}$. □

Finally we can state the injectivity result on the linearized system (3.8)–(3.9) at the exact solution.

Theorem 3.5 *Let z be the parameterization of the boundary ∂D, let ψ_1, ψ_2 solve (2.20)–(2.21) for a nonnegative $\lambda \in C[0,\pi]$ and for linearly independent Dirichlet data f_1 and f_2 such that the corresponding single-layer potentials satisfy the condition (3.3). Assume that ζ is of the form given in Lemma 3.2 and that $\chi_1, \chi_2 \in L^2[0,2\pi]$, $\mu \in C[0,\pi]$ and ζ solve the homogeneous system*

$$\begin{aligned} \widetilde{S}(\chi_i,z) + d\widetilde{S}(\psi_i,z;\zeta) = 0 \quad &\text{on } [\pi,2\pi], \\ \widetilde{K}'(\chi_i,z) + d\widetilde{K}'(\psi_i,z;\zeta) = 0 \quad &\text{on } [\pi,2\pi] \end{aligned} \tag{3.24}$$

and

$$\begin{aligned} \widetilde{K}'(\chi_i,z) + d\widetilde{K}'(\psi_i,z;\zeta) + \lambda\widetilde{S}(\chi_i,z) \\ +\lambda d\widetilde{S}(\psi_i,z;\zeta) + \mu\widetilde{S}(\psi_i,z) = 0 \quad \text{on } [0,\pi]. \end{aligned} \tag{3.25}$$

Then $\chi_1 = \chi_2 = 0, \zeta = 0$ and $\mu = 0$.

Proof. The proof is analogous to that of Theorem 3.1. First from the differential equation (3.23) we conclude that $q = 0$ and from the second statement of Lemma 3.4 we observe that $\chi_1 = \chi_2 = 0$. Then, from (3.23) we have that $\mu(u_i\circ z)\,|z'| = 0$ and the proof is concluded as in Theorem 3.1 using Holmgren's theorem and the impedance boundary condition. □

Of course, the occurrence of the same ordinary differential equation in the injectivity proofs for both approaches further illuminates their close connection.

4 Numerical method and examples

For the numerical solution of the integral equations arising in the two algorithms, in principle, we propose to use the usual Nyström and collocation methods based on trigonometric interpolations for boundary value problems for the Laplace equation as described in [15]. However, because of singularities of the solution to (1.1)–(1.3) at the two intersection points, discretizing the equations with equidistant points on $[0, 2\pi]$ would lead to a poor accuracy. For this reason, it is more appropriate to use a mesh that is graded towards the intersections points. Such a grading can be achieved most efficiently by using a sigmoidal transformation, i.e., a strictly monotonically increasing function $\omega : [0, 2\pi] \to [0, 2\pi]$ with the derivatives vanishing up to a certain order $p-1$, $p \geq 2$, at the two intersection points $t = 0$ and $t = \pi$. For details we refer to [5, 6, 14] and note that the discretization is obtained by replacing the parameterization z in the integral operators by $\widetilde{z} = z \circ \omega$ and then discretizing on an equidistant mesh.

The synthetic data were obtained by reversing the roles of f and g and, given f, interpreting the integral equation of Theorem 2.1 as an integral equation of the second kind for the unknown $u|_{\partial D}$. To avoid an inverse crime we used different grading parameters, i.e., $p = 6$ for the forward problem and $p = 4$ for the inverse algorithms and twice the number of discretization points in the forward solver. In our examples the synthetic Cauchy data $(f_i, g_i), i = 1, 2$, were obtained for the Neumann conditions

$$g_1(t) = \sin^4 t, \quad g_2(t) = \cos^2 t, \quad t \in [\pi, 2\pi],$$

respectively, and with the impedance function λ on Γ_c given by

$$\lambda(t) = \sin^4 t + 1, \quad t \in [0, \pi]. \tag{4.1}$$

As boundary shapes we considered two cases: firstly, an apple-shaped smooth contour with parameterization

$$z(t) = 0.5\, \frac{0.5 + 0.4\cos t + 0.1 \sin 2t}{1 + 0.8 \cos t}\, (\cos t, \sin t), \quad t \in [0, 2\pi], \tag{4.2}$$

and, secondly, a piece-wise smooth boundary with corners at the intersection points. For the latter the upper part Γ_m is a peanut-shaped contour given by

$$z_m(t) = -\left(1 + \frac{1}{3}\, \sin t - \frac{1}{6}\, \sin 3t\right) (0.3 \cos t, 0.2 \sin t), \quad t \in [\pi, 2\pi], \tag{4.3}$$

and the lower part Γ_m is a sink-shaped contour given by

$$z_c(t) = \left(0.3\, \frac{2t - \pi}{\pi}, -0.2 \sin t\right), \quad t \in [0, \pi]. \tag{4.4}$$

In the iterative inverse algorithm at each iteration step we solve the system (3.1)–(3.2) or the system (3.8)–(3.9) approximately via Tikhonov regularization with an H^2 penalty term on ζ with regularization parameter β, an L^2 penalty term on the densities ψ_1, ψ_2 with parameter α and an H^2 penalty term on the impedance μ with parameter γ.

The potentials and densities, respectively, were discretized using $2n = 64$ grid points on each boundary part. The update ζ of the boundary part Γ_c was given by

$$\zeta = \sum_{j=1}^{N} a_j q_j \in Q_N,$$

where the basis elements of the approximation space $Q_N, N \geq 3$, were chosen as

$$q_j(t) = r_j(t)(\cos t, \sin t), \quad j = 1, \ldots, N, \quad 0 \leq t \leq \pi,$$

with radial parts

$$r_1(t) = t(\pi - t)^2, \quad r_2(t) = t^2(\pi - t)$$

and

$$r_j(t) = \sin(j-2)t, \quad j = 3, \ldots, N.$$

In the examples we choose $N = 10$.

We started the iterations with an initial approximation for Γ_c given by the half circle in the lower half plane with end points coinciding with the end points $z(\pi)$ and $z(2\pi)$ of Γ_m and with an initial approximation for λ given by a constant. In our examples we used different constants $\lambda_{\text{initial}} \in \{3, 5, 10\}$. For the approximation space of the impedance function we choose the space of trigonometric polynomials of degree less than or equal to $L = 4$.

We performed 30 iteration steps and present reconstructions after 1, 5 and 10 steps in Figures 4.1–4.4. In Figure 4.4 we also show the reconstructions using Green's theorem approach after the 30th iteration since the results could still be improved after the first 10 steps. The exact boundary curve and impedance function are represented by the full lines and the reconstructions by dotted lines for one iteration, the dash-dotted lines for five iterations, the dashed lines for ten iterations and the initial guess is given by the sparsely dotted curve. The regularization parameters were chosen by trial and error and are presented in Table 4.1.

		Green's theorem			Potential		
Γ_c	λ_{initial}	α	β	γ	α	β	γ
(4.4)	5	10^{-9}	10^{-3}	10^{-7}	10^{-9}	10^{-4}	10^{-7}
	10	10^{-9}	10^{-4}	10^{-8}	10^{-8}	10^{-4}	10^{-7}
(4.2)	3	10^{-7}	10^{-4}	10^{-6}	10^{-9}	10^{-4}	10^{-7}
	5	10^{-8}	10^{-3}	10^{-6}	10^{-9}	10^{-4}	10^{-7}

Table 4.1: Regularization parameters

In Table 4.2 the relative L^2-error between the true impedance function and its reconstruction is presented for both contours and various initial approximations for λ after a certain number of iteration steps. Furthermore, Table 4.3 shows the smallest relative L^2-error before it started to increase and the number of iterations needed to reach this error level.

Based on these examples and further numerical experiments we can observe that, in general, the potential approach produces good reconstructions in fewer iterations than the Green's theorem approach. Furthermore it can be seen that the potential approach shifts the initial guess of the impedance function immediately to the correct level whereas the Green's theorem approach first moves it to zero and thereafter to the correct level.

To also illustrate the stability of both methods we have generated 10 sets of noisy data with noise of the form

$$g^\delta := g + \delta \frac{\|g\|_{L^2}}{\|\eta\|_{L^2}} \eta$$

added to the Neumann data where g is the unperturbed data, η is a normally distributed random variable and δ is the relative noise level. As an example we consider the apple-shaped contour (4.2) and the impedance function (4.1). As initial approximation for the boundary we took the lower half-circle as above and for the impedance we have chosen the constant $\lambda_{\text{initial}} = 5$. The regularization parameters are given in Table 4.4.

Figure 4.5 shows the best and the worst reconstructions with respect to the relative L^2-error between the reconstructed and the true impedance function. Here, we used the noise level $\delta = 0.03$. In Figure 4.6 the same is shown for the noise level $\delta = 0.06$. For the purpose of illustration, although this is not practical, the iterations were stopped as soon as the L^2-error started to increase. The actual errors and numbers of iterations are presented in Table 4.5.

The dash-dotted lines show the best reconstruction and the dotted lines the least accurate reconstruction. The solid lines represent the exact boundary and impedance, respectively. The initial approximations are again given by the dotted

Γ_c	λ_{initial}	iterations	Relative L^2 error	
			Green's theorem	Potential
(4.4)	5	5	0.0811	0.0533
		10	0.0737	0.0648
		30	0.0779	0.0761
	10	5	0.2667	0.0179
		10	0.1115	0.0191
		30	0.1053	0.0350
(4.2)	3	5	0.0844	0.0537
		10	0.0825	0.0529
		30	0.0785	0.0551
	5	5	0.1419	0.0792
		10	0.0605	0.0782
		30	0.0550	0.0804

Table 4.2: Relative L^2-error between true and reconstructed impedance

Γ_c	λ_{initial}	Green's theorem		Potential	
		least L^2-error	iterations	least L^2-error	iterations
(4.4)	5	0.0726	7	0.0451	3
	10	0.0202	15	0.0175	7
(4.2)	3	0.0785	30	0.0529	12
	5	0.0515	13	0.0780	8

Table 4.3: Smallest relative L^2-error between true and reconstructed impedance

curves. For perturbed Neumann data with 3% and 6% noise we achieved fairly good reconstructions. However, with noise levels above 6% the accuracy of the reconstructions deteriorated.

We can summarize that both approaches show accurate reconstructions with a reasonable stability against noisy data. Only a few iterations are needed to obtain good reconstructions. Furthermore, it seems that the potential approach does not depend as crucially on a good initial guess and on the choice of the regularization parameters as the Green's theorem approach. For both approaches it turned out

	Green's theorem			Potential		
noise level	α	β	γ	α	β	γ
$\delta = 0.03$	10^{-7}	10^{-2}	10^{-5}	10^{-7}	10^{-3}	10^{-5}
$\delta = 0.06$	10^{-6}	10^{-2}	10^{-4}	10^{-7}	10^{-3}	10^{-5}

Table 4.4: Regularization parameters for noisy data

		Green's theorem		Potential	
noise level		rel. L^2-error	iterations	rel. L^2-error	iterations
$\delta = 0.03$	least	0.1603	5	0.1074	3
	highest	0.3242	6	0.2832	3
$\delta = 0.06$	least	0.0644	15	0.1564	2
	highest	0.6196	2	0.3412	3

Table 4.5: Relative L^2-error between true and reconstructed impedance for different noise levels

that, in general, a smaller regularization parameter can be taken for the densities in comparison to that for the boundary and the impedance.

Acknowledgments

The research of C.S. was supported by the German Research Foundation DFG through the Graduiertenkolleg *Identification in Mathematical Models*. Part of the research was done while C.S. was visiting the University of Delaware. The hospitality and the support are gratefully acknowledged.

References

[1] S. Andrieux, T. Baranger, and A. B. Abda. Solving Cauchy problems by minimizing an energy-like functional. *Inverse problems*, 22:115–133, 2006.

[2] V. Bacchelli. Uniqueness for the determination of unknown boundary and impedance with the homogeneous Robin condition. *Inverse Problems*, 25(1):4, 2009.

[3] F. Cakoni, D. Colton, and P. Monk. The direct and inverse scattering problem for partially coated obstacles. *Inverse Problems*, 17:1997–2015, 2001.

[4] F. Cakoni and R. Kress. Integral equations for inverse problems in corrosion detection from partial Cauchy data. *Inverse Problems and Imaging*, 1:229–245, 2007.

[5] F. Cakoni, R. Kress and C. Schuft. Integral equations for shape and impedance reconstruction in corrosion detection. *Inverse Problems* 26:095012, 2010.

[6] D. Colton, and R. Kress. *Inverse acoustic and electromagnetic scattering theory*, vol. 93 of Applied Mathematical Sciences, Springer-Verlag, Berlin, second edition, 1998.

[7] M. Costabel and M. Dauge. A singularly perturbed mixed boundary value problem. *Comm. Partial Differential Equations*, 21:1919–1949, 1996.

[8] D. Fasino and G. Inglese. Recovering nonlinear terms in an inverse boundary value problem for Laplace's equation: a stability estimate. *J. Comput. Appl. Math.*, 198(2):460–470, 2007.

[9] G. Hsiao and W. Wendland. On the integral equation method for the plane mixed boundary value problem of the Laplacian. *Math. Methods Appl. Sci.*, 1:265–321, 1979.

[10] G. Inglese. An inverse problem in corrosion detection. *Inverse Problems*, 13:977–994, 1997.

[11] P. G. Kaup and F. Santosa. Nondestructive evaluation of corrosion damage using electrostatic measurements. *J. Nondestructive Eval.*, 14:127–136, 1995.

[12] P. G. Kaup, F. Santosa, and M. Vogelius. Method for imaging corrosion damage in thin plates from electrostatic data. *Inverse Problems*, 12:279–293, 1996.

[13] A. Kirsch. *An Introduction to the Mathematical Theory of Inverse Problems.* Springer Verlag, 1996.

[14] R. Kress. A Nyström method for boundary integral equations in domains with corners. *Numer. Math.*, 58, 145–161 (1990).

[15] R. Kress. *Linear Integral Equations.* Springer Verlag, New York - Berlin - Heidelberg, second edition, 1999.

[16] R. Kress and W. Rundell. Nonlinear integral equations and the iterative solution for an inverse boundary value problem. *Inverse Problems*, 21:1207–1223, 2005.

[17] W. McLean. *Strongly Elliptic Systems and Boundary Integral Equations*. Cambridge University Press, Cambridge, 2000.

[18] C. D. Pagani and D. Pierotti. Identifiability problems of defects with the Robin condition. *Inverse Problems*, 25:055007, 2009.

[19] R. Potthast. Fréchet differentiability of boundary integral operators in inverse acoustic scattering. *Inverse Problems*, 10:431–447, 1994.

[20] W. Rundell. Recovering an obstacle and its impedance from Cauchy data. *Inverse Problems*, 24:045003, 2008.

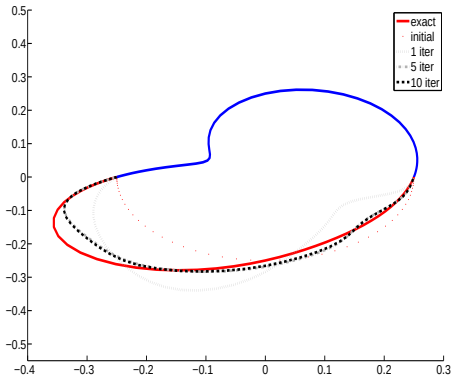

(a) Shape from Green's theorem approach

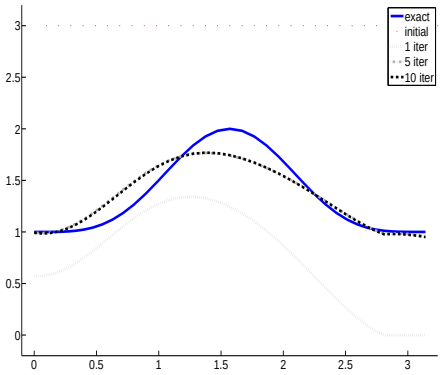

(b) Impedance from Green's theorem approach

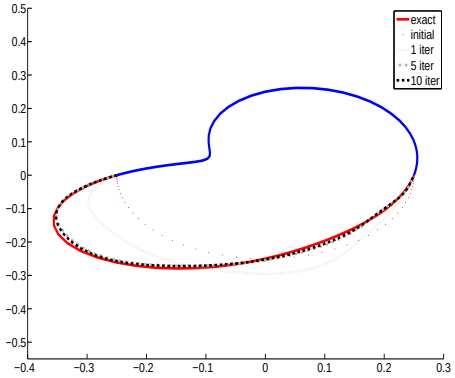

(c) Shape from potential approach

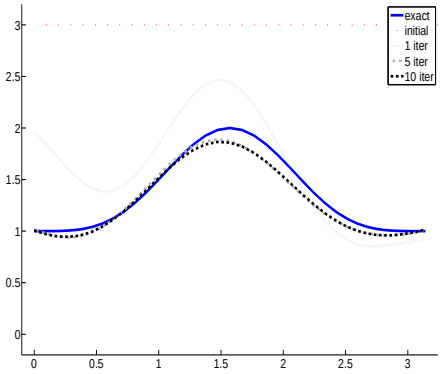

(d) Impedance from potential approach

Figure 4.1: Reconstruction of shape (4.2) and impedance (4.1) with $\lambda_{\text{initial}} = 3$

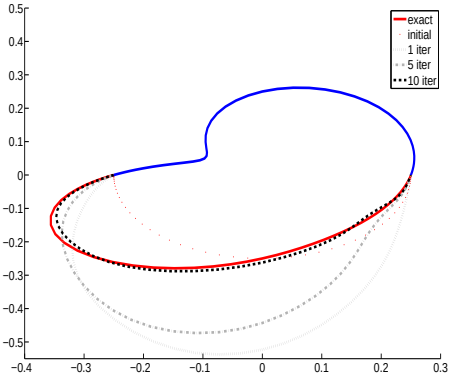

(a) Shape from Green's theorem approach

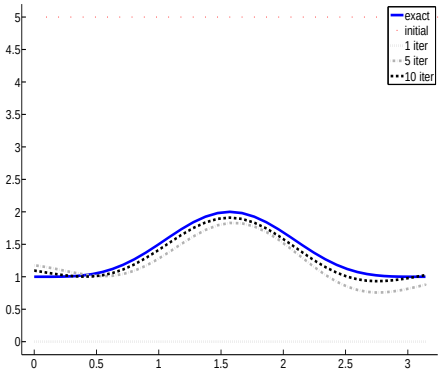

(b) Impedance from Green's theorem approach

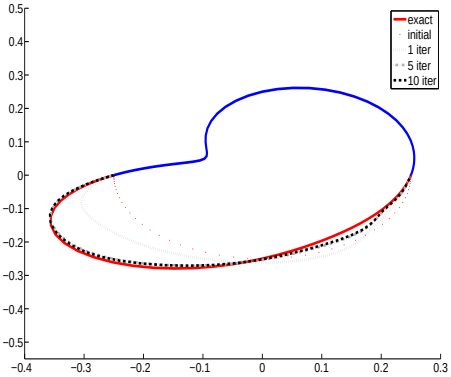

(c) Shape from potential approach

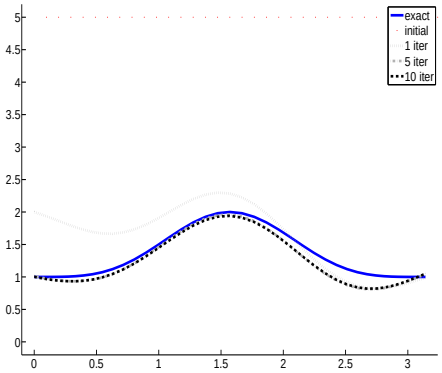

(d) Impedance from potential approach

Figure 4.2: Reconstruction of shape (4.2) and impedance (4.1) with $\lambda_{\text{initial}} = 5$

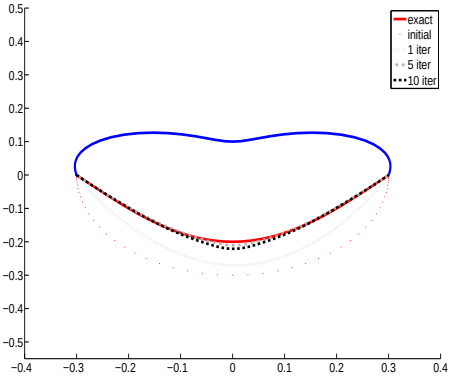

(a) Shape from Green's theorem approach

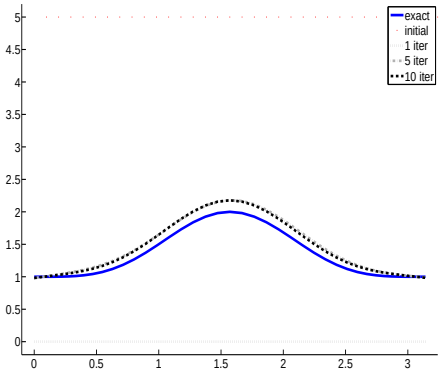

(b) Impedance from Green's theorem approach

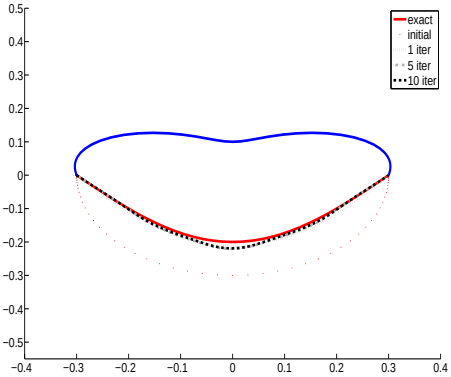

(c) Shape from potential approach

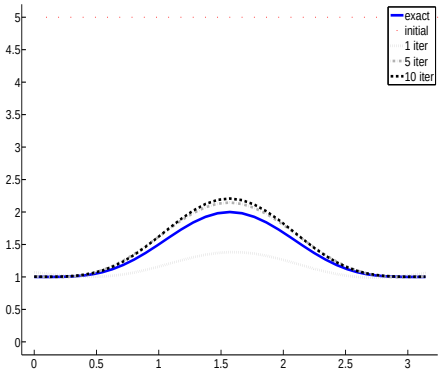

(d) Impedance from potential approach

Figure 4.3: Reconstruction of shape (4.4) and impedance (4.1) with $\lambda_{\text{initial}} = 5$

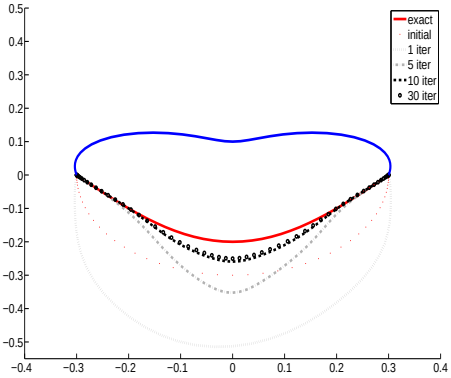

(a) Shape from Green's theorem approach

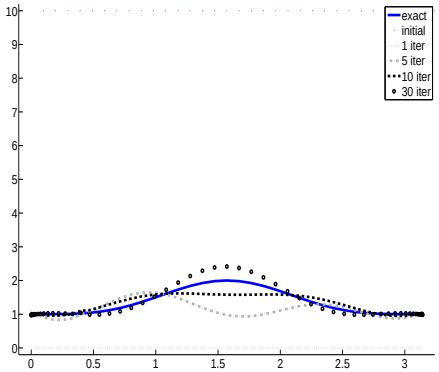

(b) Impedance from Green's theorem approach

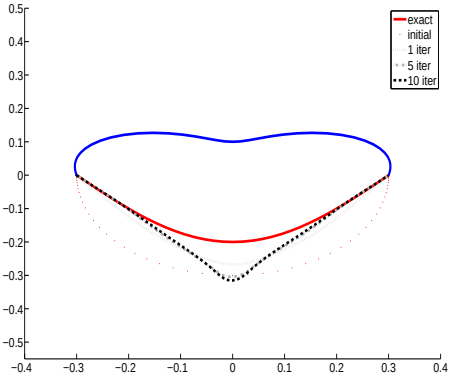

(c) Shape from potential approach

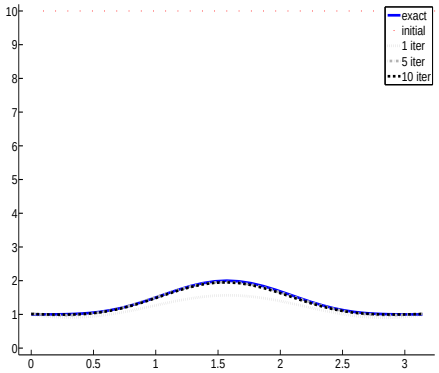

(d) Impedance from potential approach

Figure 4.4: Reconstruction of shape (4.4) and impedance (4.1) with $\lambda_{\text{initial}} = 10$

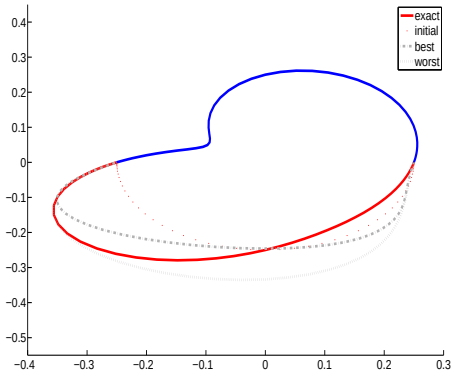

(a) Shape from Green's theorem approach

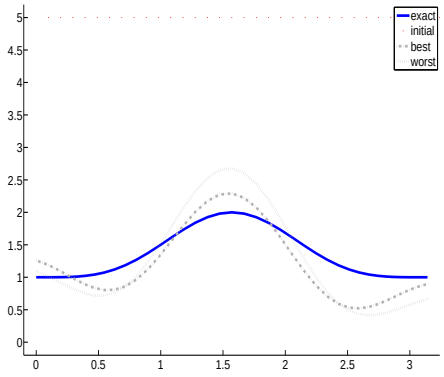

(b) Impedance from Green's theorem approach

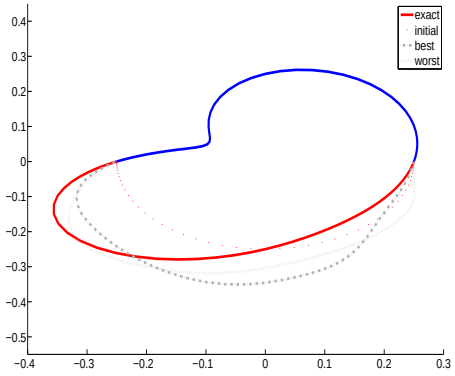

(c) Shape from potential approach

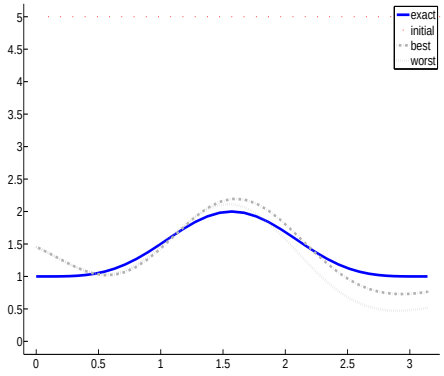

(d) Impedance from potential approach

Figure 4.5: Reconstruction of shape (4.2) and impedance (4.1) with $\lambda_{\text{initial}} = 5$ and 3% noise

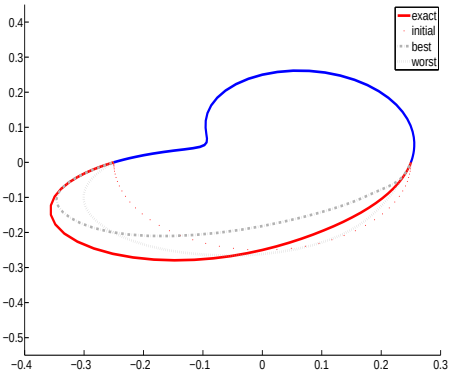

(a) Shape from Green's theorem approach

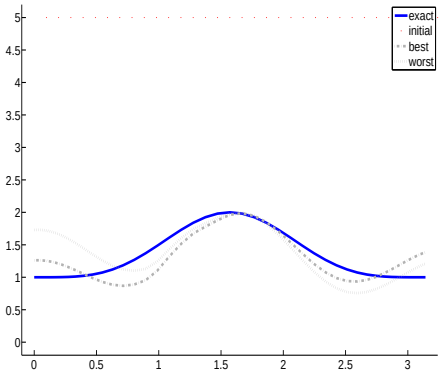

(b) Impedance from Green's theorem approach

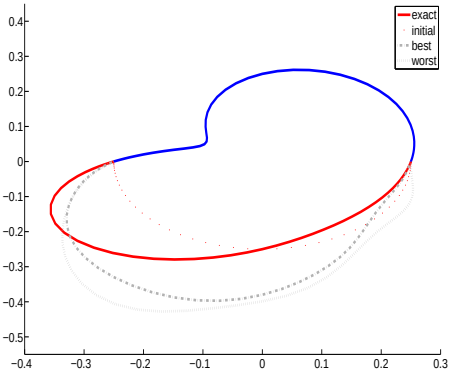

(c) Shape from potential approach

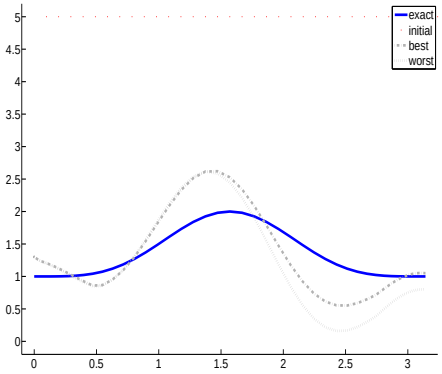

(d) Impedance from potential approach

Figure 4.6: Reconstruction of shape (4.2) and impedance (4.1) with $\lambda_{\text{initial}} = 5$ and 6% noise